

# A NEW STABILIZED ZERO - CROSSING REPRESENTATION IN THE WAVELET TRANSFORM DOMAIN AND ITS APPLICATION TO IMAGE PROCESSING

*Shinji Watanabe, Takashi Komatsu and Takahiro Saito*

Department of Electrical Engineering, Kanagawa University

3-27-1 Rokkakubashi, Kanagawa - ku, Yokohama, 221, Japan

Tel: +81 45 481 5661 Ext. 3119; fax: +81 45 491 7915; e-mail: kurikuri@cc.kanagawa-u.ac.jp

## ABSTRACT

We present a new stabilized zero-crossing representation with a salient feature that the signal reconstruction problem reduces to a typical minimum-norm optimization problem, the solution of which is formulated as a linear simultaneous equation, and develop an iterative algorithm for signal reconstruction. Moreover, we extend them to the two-dimensional case. Furthermore, we introduce a threshold operation based on edge intensity to reduce the amount of information in the stabilized zero-crossing representation, and experimentally demonstrate that the threshold operation works well.

## 1 INTRODUCTION

Many previous studies have proved that multiscale zero-crossing representations are well adapted for extracting local important features such as edges from images. The justifiability of multiscale zero-crossing representations originate in the Logan's theorem [1]. The multiscale zero-crossing representation is complete, but not stable in the sense that a small perturbations of the representation may correspond to an arbitrary large perturbation of the original signal.

To stabilize the reconstruction of a signal from its zero-crossings, recently Mallat has developed the stabilized waveform representation based on both zero-crossings of a dyadic multi-scale wavelet transform with the property of local second derivative operation and additional information such as the value of the wavelet transform integral between two zero-crossings, and he conjectured that the stabilized zero-crossing waveform representation might be complete and stable [2]. In addition, he has formed an algorithm for reconstructing signals from the stabilized zero-crossing representation. The Mallat's signal reconstruction algorithm based on the POCS (projections onto convex sets) formulation iterates on a nonexpansive projection onto a convex set and an orthogonal projection onto a Hilbert subspace, and hence the convergence is guaranteed. Since then, many studies have described variants of a stabilized zero-crossing waveform representation. For instance, some studies have analyzed the variant which as a complement of information uses a position and amplitude of each local extremum that is defined as maximum absolute value lying between two consecutive zero-crossings [3]. For almost all the variants presented so far, signal reconstruction problems have been formulated as a non-linear optimization problem, and the resultant signal reconstruction algorithms are based

on the POCS formulation like the Mallat's reconstruction algorithm. With the POCS-based alternate projection algorithms we can reconstruct signal waveform from the stabilized zero-crossing representation with high fidelity.

These types of zero-crossing representation is considered almost complete, but they have common drawbacks. The first drawback is that it is neither straightforward nor trivial to extend their signal reconstruction algorithms from one-dimensional signal to two-dimensional signals. The difficulty of the extension results from the non-linearity of the reconstruction problems. The second drawback is that for almost complete signal reconstruction the positions of zero-crossings and/or local extrema should be represented with fractional sampling interval accuracy, which makes it difficult to apply the stabilized zero-crossing representations to practical image processing. The third drawback is that the POCS-based alternate projection algorithms for signal reconstruction involve a large amount of computational efforts.

To cope with the above-mentioned drawbacks, we present a new stabilized two-dimensional zero-crossing representation in the wavelet transform domain. For the new stabilized zero-crossing representation, we represent the positions of zero-crossings as a certain sampling point, and to stabilize the representation we add a complement of information that is defined as an inner product between an original signal and an integrated basis function of the dilated and shifted basic wavelet function at each zero-crossing point. The new stabilized zero-crossing representation has a salient feature that the problem of how to reconstruct signals from it reduces to a typical minimum-norm optimization problem, the solution of which is formulated as a linear simultaneous equation [4]. However, the dimension of the resultant linear simultaneous equation is very large, and hence we employ an iterative relaxation method for solving the simultaneous equation.

## 2 WAVELET TRANSFORM

The wavelet transform is performed by applying dilation and translation to a basic wavelet function  $\psi(\bullet)$  and then estimating an inner product between a given input signal  $f(\bullet)$  and the distorted wavelet function:

$$W_a(b) = \frac{1}{\sqrt{a}} \cdot \int \psi^* \left( \frac{x-b}{a} \right) \cdot f(x) dx \quad (1)$$

When we set  $a = 2^j$ ,  $b = n$ , where  $j$  and  $n$  are integers,  $W_a(b)$

) is reduced to the discrete wavelet transform with the shift invariant property. We refer to this type of wavelet transform as dyadic multiscale wavelet transform. The dyadic multiscale wavelet transform is more redundant than the usual standard discrete wavelet transform where  $a = 2^j$ ,  $b = n \times 2^j$ .

The dyadic multiscale wavelet transform has the perfect reconstruction property that an original signal is perfectly reconstructed from the wavelet transforms at all the scales  $j = 1, 2, \dots$ , but it is not feasible to use the wavelet transforms at all the scales. Instead, we limit the scale  $j$  within the range  $j = 1, 2, \dots, M$ , and reconstruct an original signal from both the wavelet transforms at the scales  $j = 1, 2, \dots, M$  and the smoothed signal at the coarsest scale  $j = M$ .

In this paper we use a basic wavelet function  $\psi(\bullet)$  which is defined as a second derivative of a short-length smoothing function and forms a bi-orthogonal basis with the properties of the linear phase and the local second derivative operation. In this case, the detection of zero-crossing points corresponds to the extraction of edges. In order to reduce the detection of false zero-crossing points caused by ripples of the basic wavelet function, we employ a short-length smoothing function derived from the B-spline function [3]. The unit impulse responses  $h_L(\bullet)$ ,  $h_H(\bullet)$  of the band-splitting low-pass and high-pass filters used for the dyadic multiscale wavelet transform with the second derivative operation are as follows:

- (a) Low-pass analysis filter :
- $$\{ h_L(1) = 0.25, h_L(0) = 0.50, h_L(-1) = 0.25 \}$$
- (b) High-pass analysis filter :
- $$\{ h_H(1) = -0.25, h_H(0) = 0.50, h_H(-1) = -0.25 \}$$

### 3 ZERO - CROSSING REPRESENTATION

In the new stabilized zero-crossing representation, we represent the position  $Z_i$  of each zero-crossing point with integral sampling interval accuracy, that is to say, for the true position of each zero-crossing point we substitute the sampling point which is nearest to the true position. In order to stabilize the reconstruction of a signal from its zero-crossings, we add a complement of information that is defined as an inner product  $P_i$  between an original signal  $f(x)$  and an integrated function  $\sigma_j(x; Z_i)$  of the dilated and shifted basic wavelet function  $\psi((x - Z_i) / 2^j)$  at the position  $Z_i$  of each zero-crossing point:

$$P_i = \left\langle f(x), \sigma_j(x; Z_i) \right\rangle \quad (2)$$

$$\sigma_j(x; Z_i) \equiv \frac{1}{N} \cdot \int_{-\infty}^x \psi\left(\frac{t - Z_i}{2^j}\right) dt \quad (3)$$

where  $N$  is the normalization factor.

When we use a basic wavelet function  $\psi(\bullet)$  with the second derivative property, the inner product defined by Eq. 2 corresponds to applying a first derivative operation to an original signal  $f(\bullet)$ . Moreover, the definition of the integrated basis function  $\sigma_j(\bullet)$  is obtained by applying wavelet transformation to a unit step function  $U(\bullet)$ ; hence the function  $\sigma_j(\bullet)$  serves as an edge model function and the value of the inner product  $P_i$  corresponds to intensity of the

edge model function included in an original signal  $f(\bullet)$ .

### 4 SIGNAL RECONSTRUCTION

The problem of how to reconstruct signals from the new stabilized zero-crossing representation reduces to a typical minimum-norm optimization problem where a vector with a minimum norm is selected as an optimal solution vector under the constraint that inner products of a solution vector with the multiple basis vectors are given. The solution of the minimum-norm optimization problem is easily formulated as a linear simultaneous equation. In the case of the signal reconstruction problem, however, the dimension of the resultant linear simultaneous equation is equal to the number of detected zero-crossings, and too large to solve the equation directly, non-iteratively. Instead, we employ an iterative relaxation method for solving the equation. The mathematical theory for linear operators guarantees that the iterative signal reconstruction algorithm has the convergence property.

The iterative signal reconstruction algorithms is as follows.

#### [ Iterative Signal Reconstruction Algorithm ]

- (1) Adopt a smoothed signal at the coarsest scale  $j = M$  as an initial function of a reconstruction signal  $R(x)$ .
- (2) Apply the procedures of the steps, (2-1) and (2-2), to all the zero-crossings at all the scales.
  - (2-1) For each zero-crossing  $Z_i$  at the scale  $j$ , compute an inner product  $Q_i$  between the present reconstruction signal  $R(x)$  and the integrated basis function  $\sigma_j(x; Z_i)$ .
  - (2-2) Update the reconstruction signal  $R(x)$  as follows:
$$R(x) \leftarrow R(x) + (P_i - Q_i) \cdot \sigma_j(x; Z_i) \quad (4)$$
- (3) Repeat the above operations of the step (2), until convergence.

### 5 EXTENSION TO TWO-DIMENSIONAL SIGNALS

We extend the new stabilized zero-crossing representation and the iterative signal reconstruction algorithm to the two-dimensional case.

For the extension, we employ the multiscale pyramidal wavelet transform as a two-dimensional multiscale wavelet transform. Firstly we decompose an input signal into four multiscale dyadic wavelet transforms  $W_{LL}(x, y)$ ,  $W_{LH}(x, y)$ ,  $W_{HL}(x, y)$ ,  $W_{HH}(x, y)$  by performing horizontal wavelet transform and vertical wavelet transform sequentially, and then we compose an objective multiscale pyramid wavelet transform  $W_H(x, y)$  by reconstructing it from only the three different wavelet transforms  $W_{LH}(x, y)$ ,  $W_{HL}(x, y)$ ,  $W_{HH}(x, y)$ . The multiscale pyramidal wavelet transform has the same data structure as the Laplacian pyramid image representation [5], and has the property of perfect reconstruction.

For a given two-dimensional signal, zero-crossings of its multiscale pyramidal wavelet transforms make zero-crossing lines. We represent the zero-crossing lines with integral sampling accuracy, that is to say, for the true zero-crossing line we substitute a sequence of the sampling points which best approximate to the true position.

Moreover, as a complement of information, at the position  $\mathbf{Z}_i = (Z_{i,x}, Z_{i,y})^t$  of each approximate zero-crossing point on the zero-crossing line at the scale  $j$ , we employ the inner product  $S_i$  between an original two-dimensional signal  $f(x, y)$  and the basis function  $\rho_j(x, y; \mathbf{Z}_i)$  which works as a first derivative operator.

$$S_i = \left\langle f(x, y), \rho_j(x, y; \mathbf{Z}_i) \right\rangle \quad (5)$$

As for the basis function  $\rho_j(x, y; \mathbf{Z}_i)$ , we prepare four different candidate functions for the basis function  $\rho_j(x, y; \mathbf{Z}_i)$  in advance, and then we select the proper function from the four candidates according to the connection of neighboring approximate zero-crossing points in the vicinity of the position  $\mathbf{Z}_i$  on the zero-crossing line. We define the four different candidate functions  $\gamma_j(x, y; \mathbf{Z}_i; n_1, n_2)$  with the two parameters  $n_1, n_2$ :

$$\begin{aligned} \gamma_j(x, y; \mathbf{Z}_i; n_1, n_2) \equiv & \\ & \frac{1}{N_{i,j}} \left\{ \eta_j(x, y; Z_{i,x}, Z_{i,y}) \cdot n_1 + \eta_j(y, x; Z_{i,y}, Z_{i,x}) \cdot n_2 \right\} \\ & , (n_1, n_2) = (1, 0), (0, 1), (1, 1), (1, -1) \\ & N_{i,j} ; \text{Normalization coefficient} \end{aligned} \quad (6)$$

$$\eta_j(u_1, u_2; Z_{i,1}, Z_{i,2}) \equiv \int_{-\infty}^{u_1} \psi\left(\frac{v - Z_{i,1}}{2^j}\right) dv \cdot e^{-\frac{(u_2 - Z_{i,2})^2}{2^{2j-2}}} \quad (7)$$

where we choose the proper set of values for the two parameters  $n_1, n_2$  from the four possible sets according to the connection of neighboring approximate zero-crossing points as follows:

- (a) Horizontal connection :  $(n_1, n_2) = (1, 0)$
- (b) Vertical connection :  $(n_1, n_2) = (0, 1)$
- (c) Diagonal connection with the upper right direction :  
 $(n_1, n_2) = (1, 1)$
- (d) Diagonal connection with the lower right direction :  
 $(n_1, n_2) = (1, -1)$

(e) Vague connection : We use the two different basis functions defined by the two sets of parameter values,  $(n_1, n_2) = (1, 0), (0, 1)$ , and compute the two different inner products with the chosen two basis functions.

The function  $\eta_j(u_1, u_2; Z_{i,1}, Z_{i,2})$  appeared in the definition of the candidate function  $\gamma_j(\bullet)$  is defined by Eq. 6. The function  $\eta_j(u_1, u_2; Z_{i,1}, Z_{i,2})$  works as a first derivative operator along the  $Z_{i,1}$ -axis, whereas it behaves as a Gaussian smoothing operator along the  $Z_{i,2}$ -axis. We introduce the Gaussian smoothing operator to suppress the noticeable blockwise artifacts in the reconstructed image.

The two-dimensional iterative signal reconstruction algorithm differs from the one-dimensional algorithm in that we choose the proper basis function for the inner product according to the connection of neighboring approximate zero-crossing points on the zero-crossing line and additionally in that in the case of vague connection we use two different basis functions and their corresponding two different inner products, but does not differ in the general outline of the iterative procedure.

The two-dimensional signal reconstruction algorithm provides an almost perfectly reconstructed image. If we measure the fidelity of signal reconstruction with the *rms* signal-to-noise ratio (*SNR*) computed with respect to the original image, the two-dimensional algorithm achieves signal reconstruction with extremely high fidelity, typically 60 dB or more. High-fidelity reconstruction with *SNR* of 55 dB or more involves a large number of iterations, typically several thousands, but the algorithm gives a reconstruction image with subjectively high picture quality even after some dozens of iterations, which is a especially preferable characteristic for its practical applications to image processing.

## 6 DATA COMPRESSION OF ZERO - CROSSING REPRESENTATION

To reduce the amount of the complementary information in the stabilized zero-crossing representation, we introduce a threshold operation based on edge intensity which is defined as the absolute value of the foregoing inner product  $S_i$  at each approximate zero-crossing point. We eliminate the complementary information for the approximate zero-crossing point whose edge intensity is below the threshold value:

$$\text{if } |S_i| < \frac{\delta_j}{j} \cdot T_r, \quad (8)$$

, then eliminate that zero-crossing point  $Z_i$

where the threshold value is dependent on the scale  $j$  and  $\delta_j$  is the maximum of the absolute value of the inner product  $S_i$  at that scale. The threshold operation makes much of coarse edges with high edge intensity and reserves them, whereas it makes little of fine edges with weak edge intensity and eliminates them.

Fig. 1 gives the value of *SNR* of the image reconstructed from the compressed zero-crossing representation after  $n$  iterations, where the number of scales  $M$  is set to 4 and the value of  $T_r$  and their corresponding data compression ratios  $C_r$  are as follows:

$$\begin{aligned} T_r = 0.05 \quad (C_r = 51.6 \%), \quad T_r = 0.20 \quad (C_r = 21.7 \%) \\ T_r = 0.50 \quad (C_r = 10.4 \%), \quad T_r = 0.80 \quad (C_r = 6.0 \%) \end{aligned}$$

Fig. 2 shows the original image, whereas Fig. 3 shows the reconstructed images. As shown in Fig. 3, as we increase the value of  $T_r$ , smear noise grows wider and clearer in the reconstructed image, and from the standpoint of picture quality the value of  $T_r$  should be set to below 0.2.

At present we are studying the application to various image processing. The target applications include restoration of true lightness under complex illumination conditions, image compression and so on. We will give a detail of its target applications at the presentation.

## 7 CONCLUSIONS

We present a new stabilized two-dimensional zero-crossing representation and an iterative reconstruction algorithm with which we can almost perfectly reconstruct an original image. Moreover, we introduce a threshold operation based on edge intensity to reduce the information amount of the zero-crossing representation, and demonstrate that it works well.

**REFERENCES**

[1] B. Logan, "Information in the zero-crossings of band pass signals", *B.S.T.J.*, vol.56, pp.487-510, 1977.  
 [2] S. Mallat, "Zero-crossings of a wavelet transform", *IEEE Trans. IT*, vol. 37, pp.1019-1033, 1991.

[3] C.K. Cheong, K. Aizawa, T. Saito, and M. Hatori, "Image reconstruction based on zero-crossing representations of wavelet transform", *IEICE Trans.*, vol.J77-A, pp.992-1005, 1994.  
 [4] D.G. Leunberger, "Optimization by vector space methods", John Wiley & Sons, Inc., 1969.  
 [5] P.J. Burt and E.H. Adelson, "The Laplacian pyramid as a compact image code", *IEEE Trans. COM*, vol.31, pp.532-540, 1983.

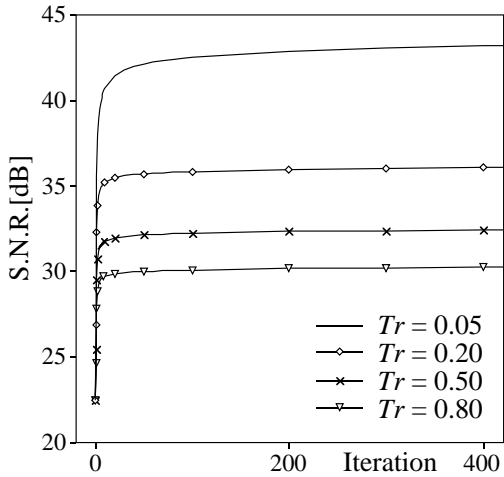


Figure 1 SNR versus the number  $n$  of iterations for image reconstruction from the compressed zero-crossing representation of the test image "Lady".



Figure 2 Original test image "Lady".



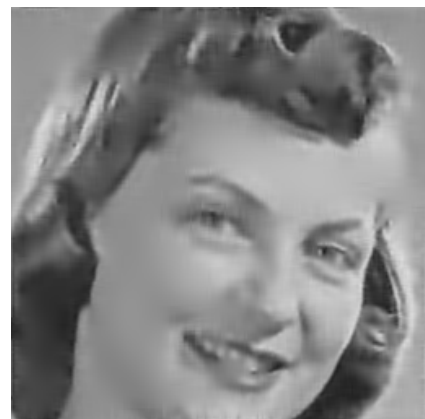
(a) Reconstructed Image ( $T_r = 0.05$ ,  $SNR = 44.2$  dB)



(b) Reconstructed Image ( $T_r = 0.20$ ,  $SNR = 36.4$  dB)



(c) Reconstructed Image ( $T_r = 0.50$ ,  $SNR = 32.6$  dB)



(d) Reconstructed Image ( $T_r = 0.80$ ,  $SNR = 30.4$  dB)

Figure 3 Reconstructed images from the compressed stabilized zero-crossing representation of the test image "Lady".